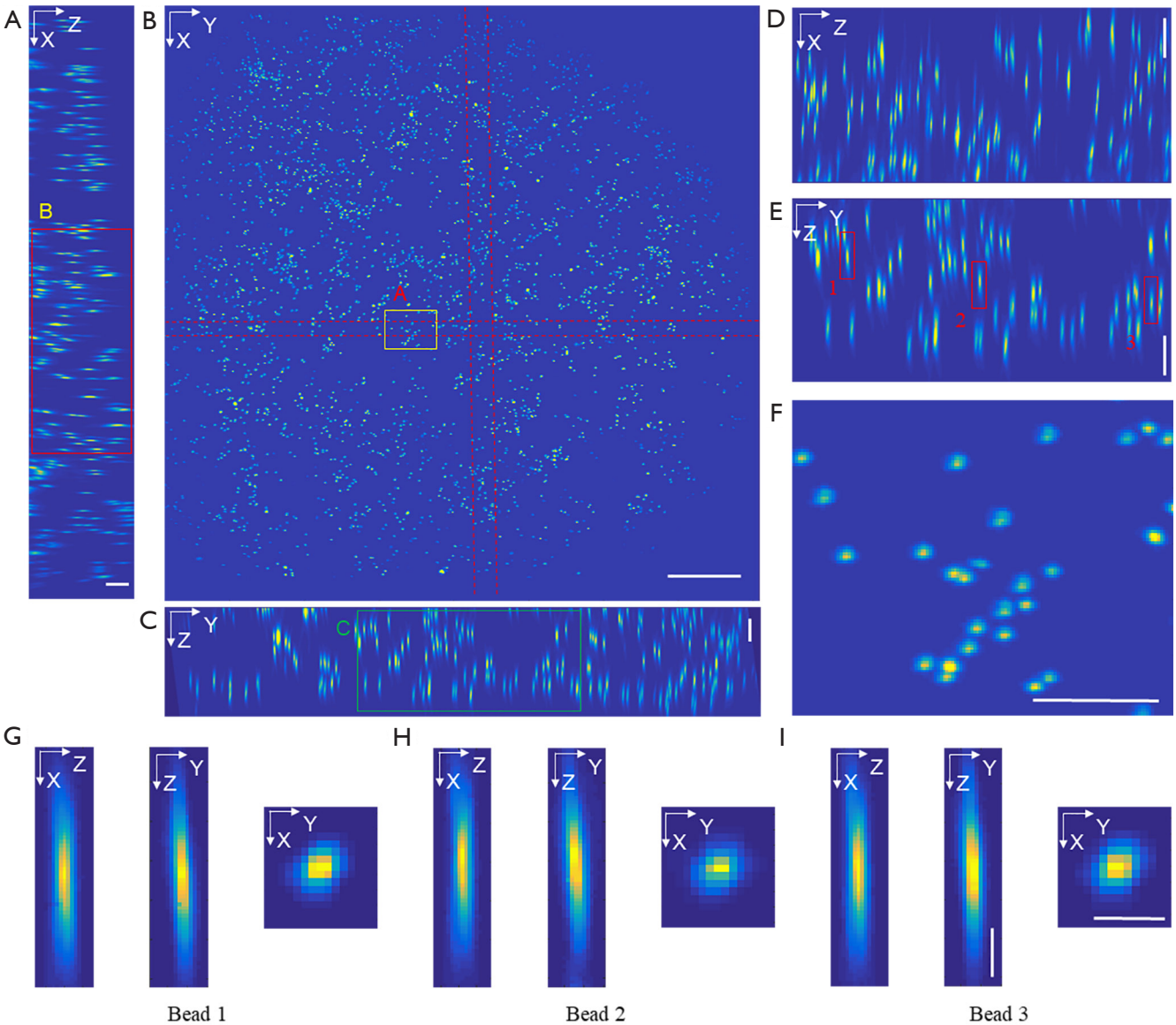

Figure S1 Resolution characterization of 20× configuration. (A-C) Maximum intensity projections of the volume along X, Y, and Z axis. The scale bar in panel (A) and (C) is 50 μm. The scale bar in panel (B) is 250 μm; (D-F) The zoom-in view of the squared area A, B, and C in panel (A-C). Both vertical and horizontal bars are 50 μm. (G-I) Axial and transversal profiles of three representative beads that are marked in panel (E). Both vertical and horizontal bars are 10 μm.

http://dx.doi.org/10.21037/qims-20-806

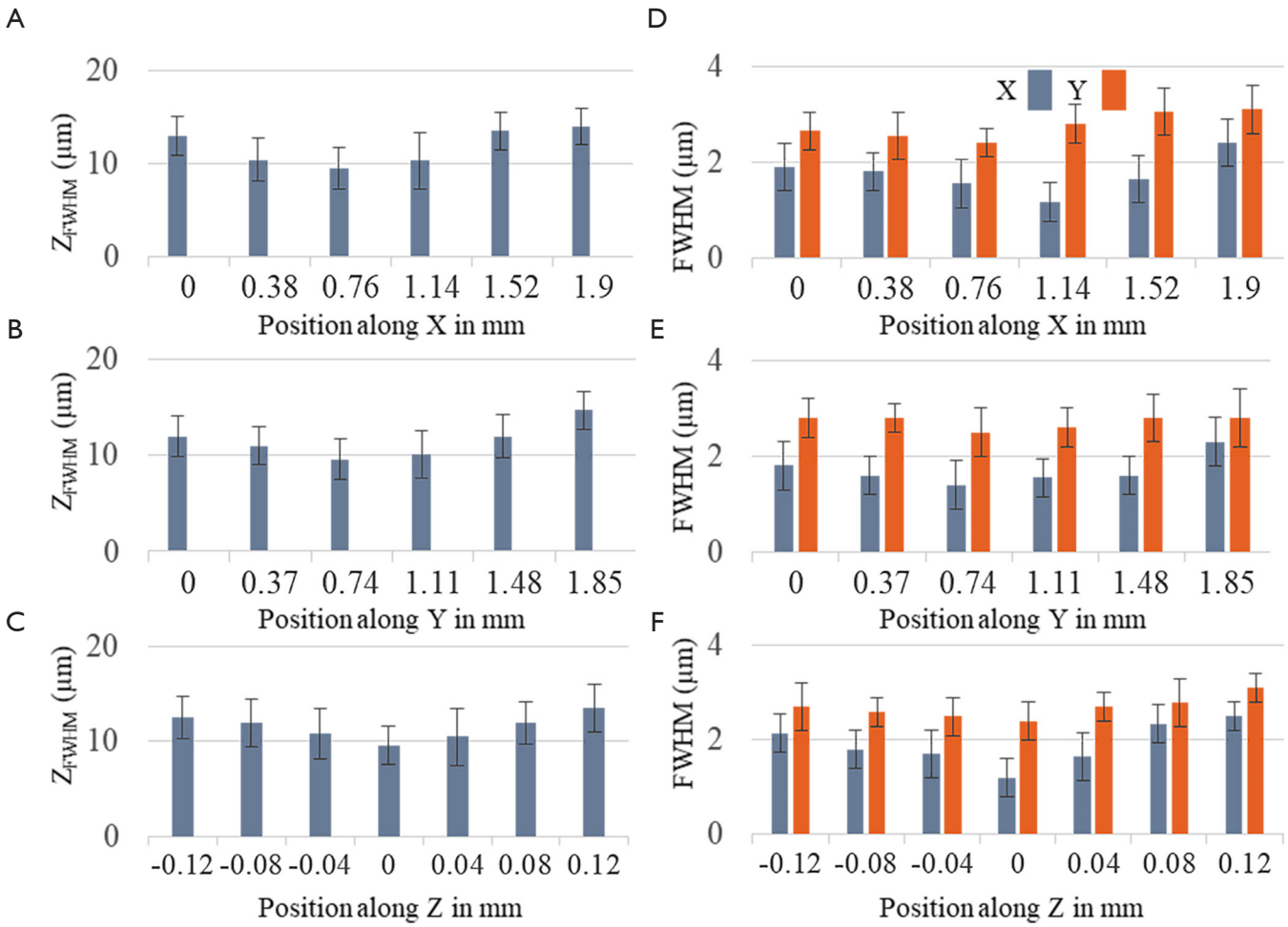

Figure S2 Resolution quantification over the full FOV. (A-C) The variation of the axial resolution along X, Y, and Z directions. (D-F) The variation of the lateral resolution along X, Y and Z directions.

http://dx.doi.org/10.21037/qims-20-806

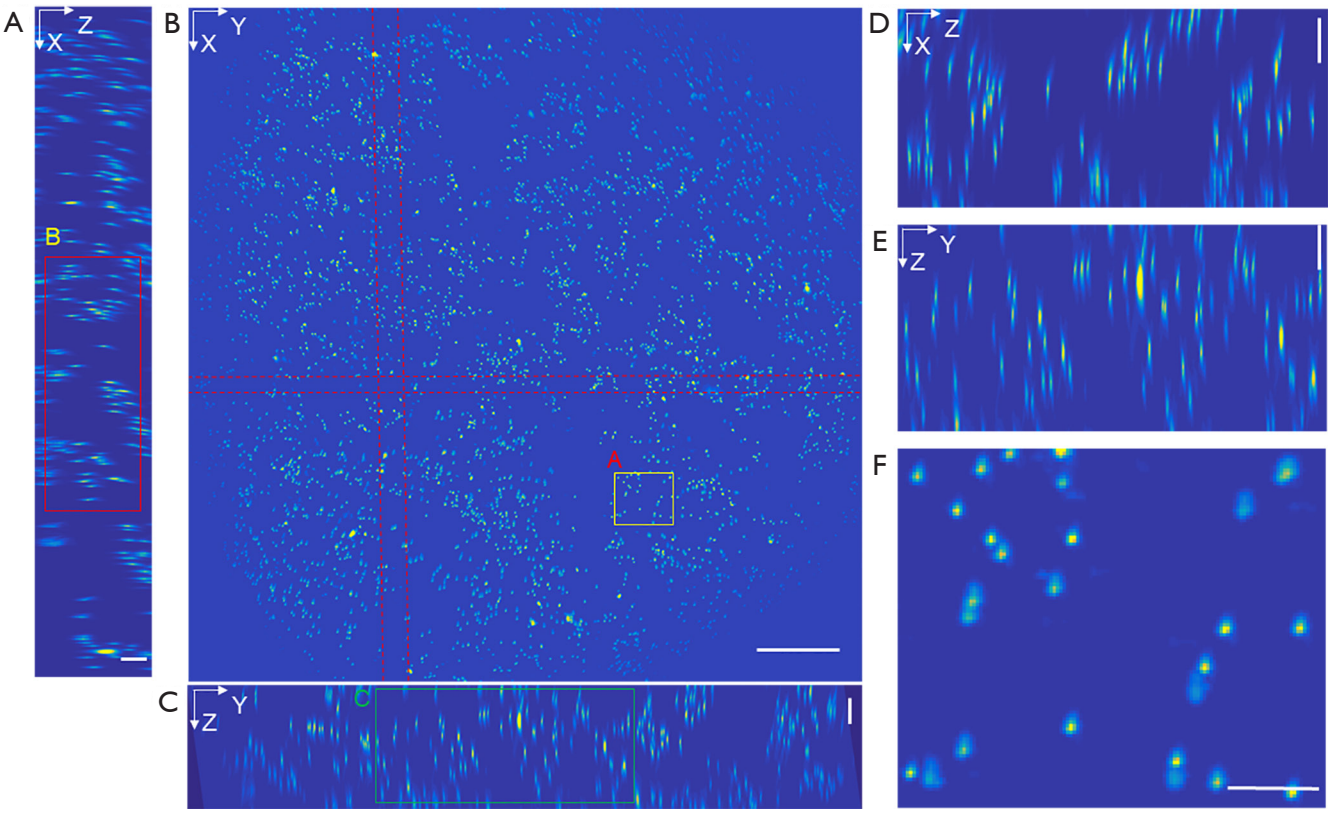

Figure S3 Different volume data were acquired under 20× configuration to prove the reproducibility of switching between different objective lenses.

http://dx.doi.org/10.21037/qims-20-806

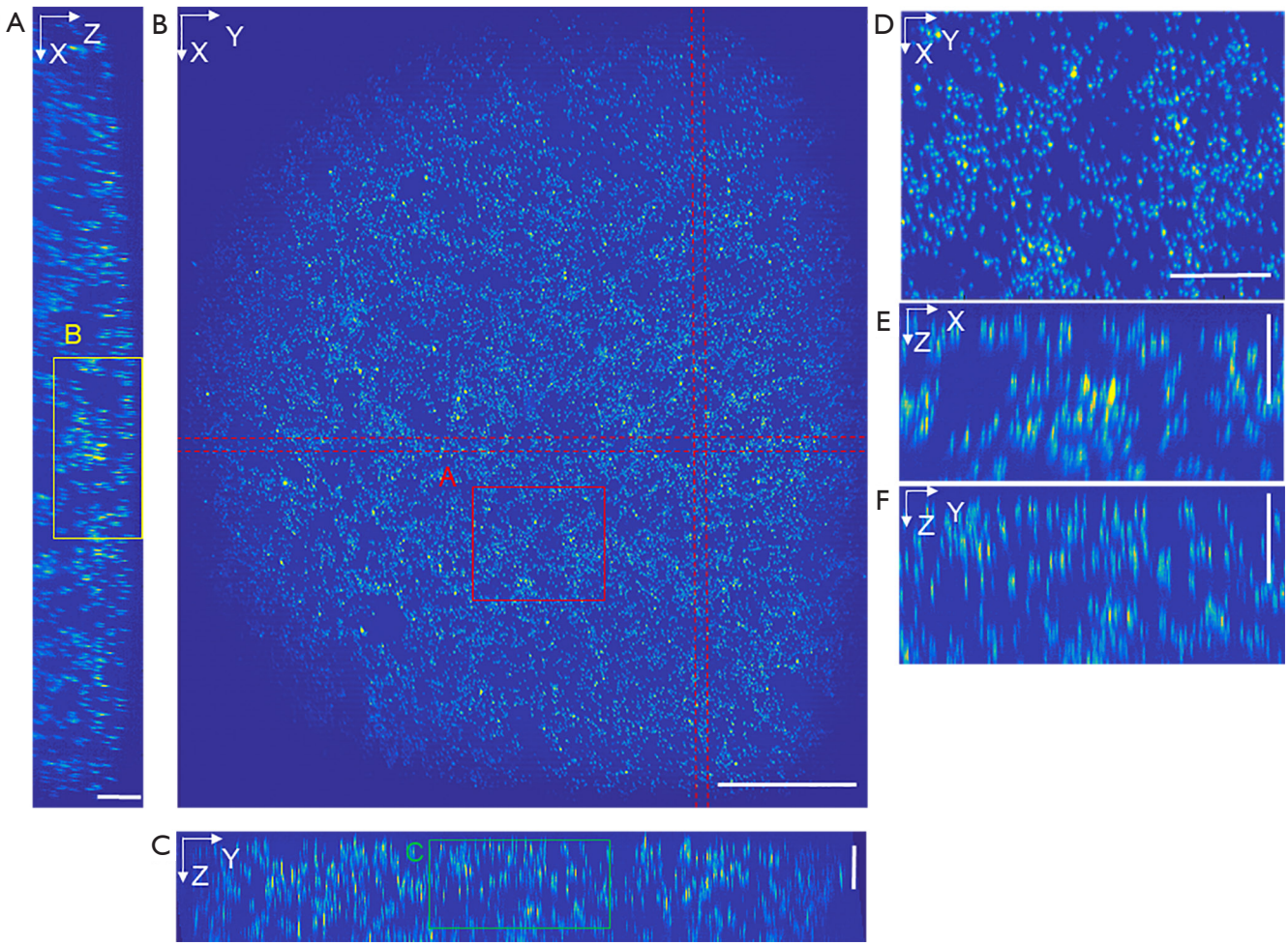

Figure S4 Different volume data were acquired under 10× configuration to prove the reproducibility of switching between different objective lenses.

http://dx.doi.org/10.21037/qims-20-806

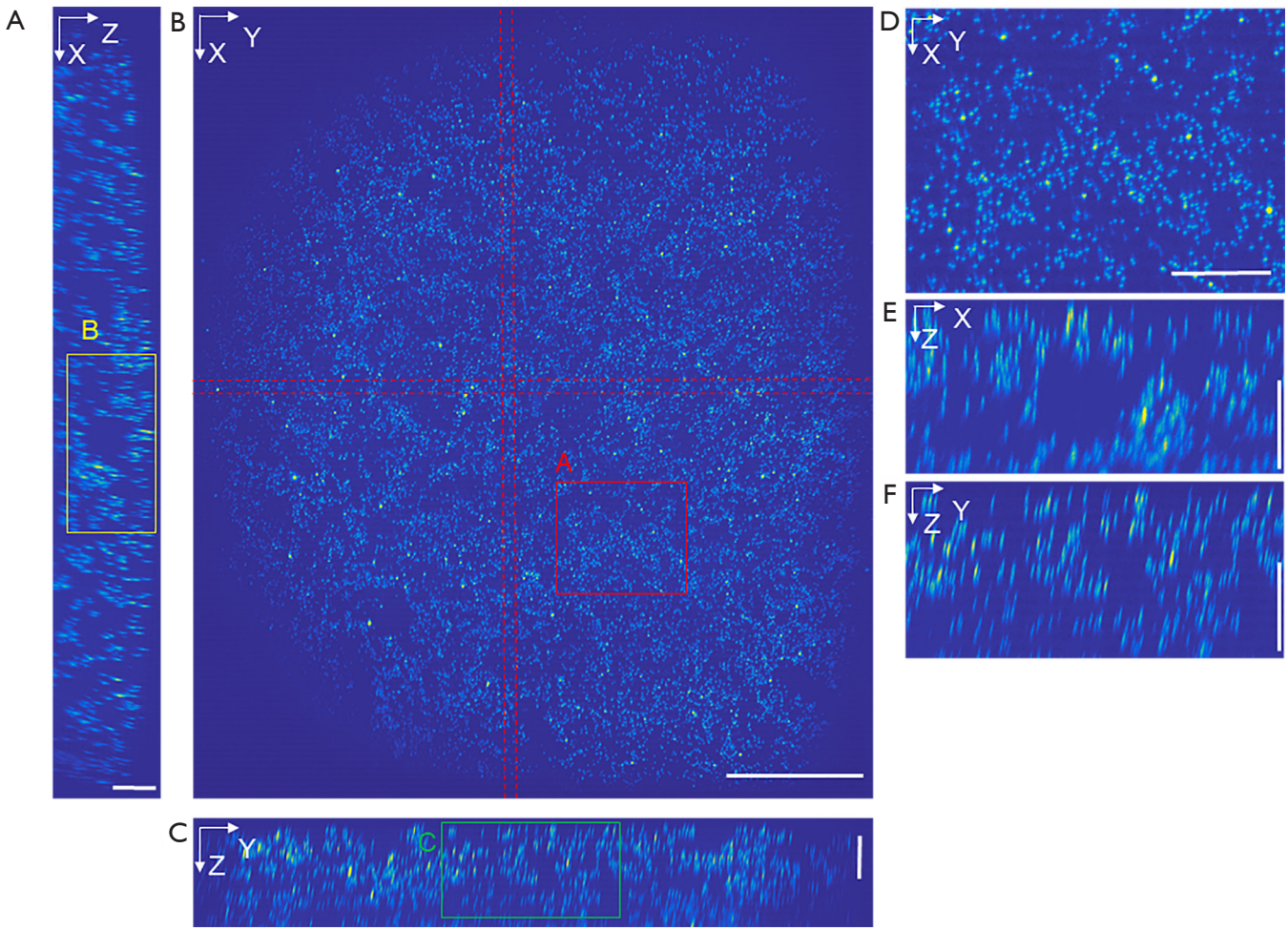

Figure S5 Cross-sectional views of beads volume acquired under 10× configuration without affine transformation. (A-C) Maximum intensity projections of the volume along X, Y, and Z axis. Scale bar in panel (A) and (C) is ~0.25 mm. Scale bar in panel (B) is ~ 1 mm; (D-F) The zoom-in view of the squared area A, B, and C in panel (A-C). Both vertical and horizontal bars are ~0.25 mm.

http://dx.doi.org/10.21037/qims-20-806

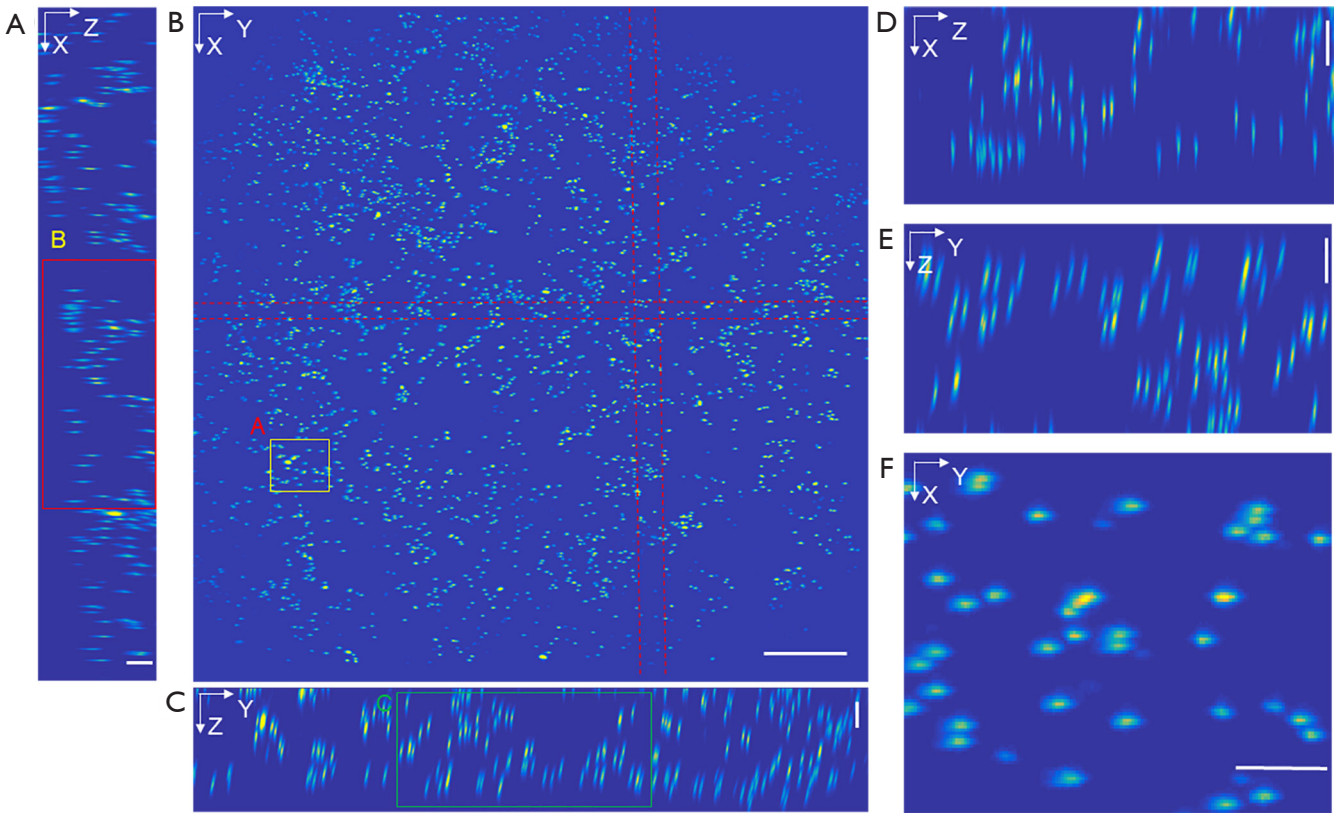

Figure S6 Cross-sectional views of beads volume acquired under 20× configuration without affine transformation. (A-C) Maximum intensity projections of the volume along X, Y, and Z axis. Scale bar in panel (A) and (C) is ~50 μm. Scale bar in panel (b) is ~250 μm; (D-F) The zoom-in view of the squared area A, B, and C in panel (A-C). Both vertical and horizontal bars are ~50 μm.

http://dx.doi.org/10.21037/qims-20-806

Figure S7 Volumetric imaging of the vasculature in a fixed mouse brain (Original data).

Figure S8 Volumetric imaging of the vasculature in a fixed mouse brain (after deconvolution process).

http://dx.doi.org/10.21037/qims-20-806

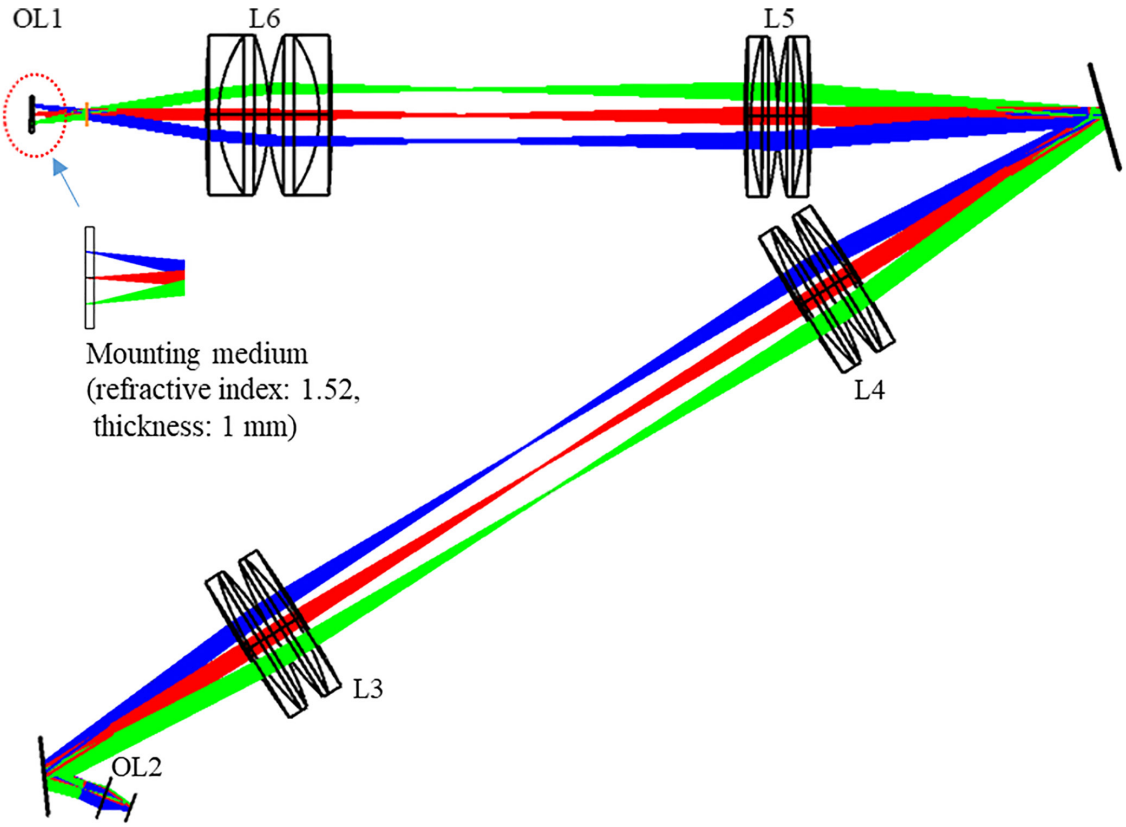

Figure S9 The layout of the Zemax simulation from OL1 to OL2.

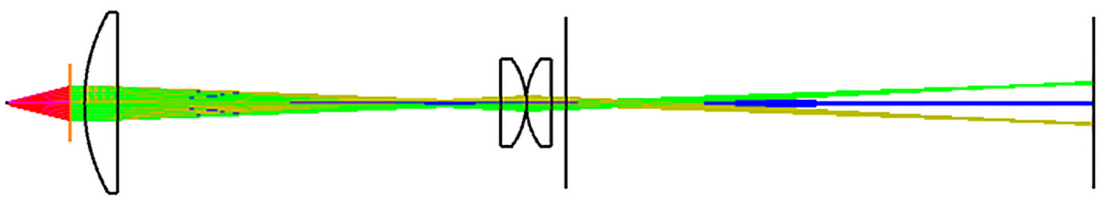

Figure S10 The layout of the remote imaging system from OL3 to L9.

http://dx.doi.org/10.21037/qims-20-806

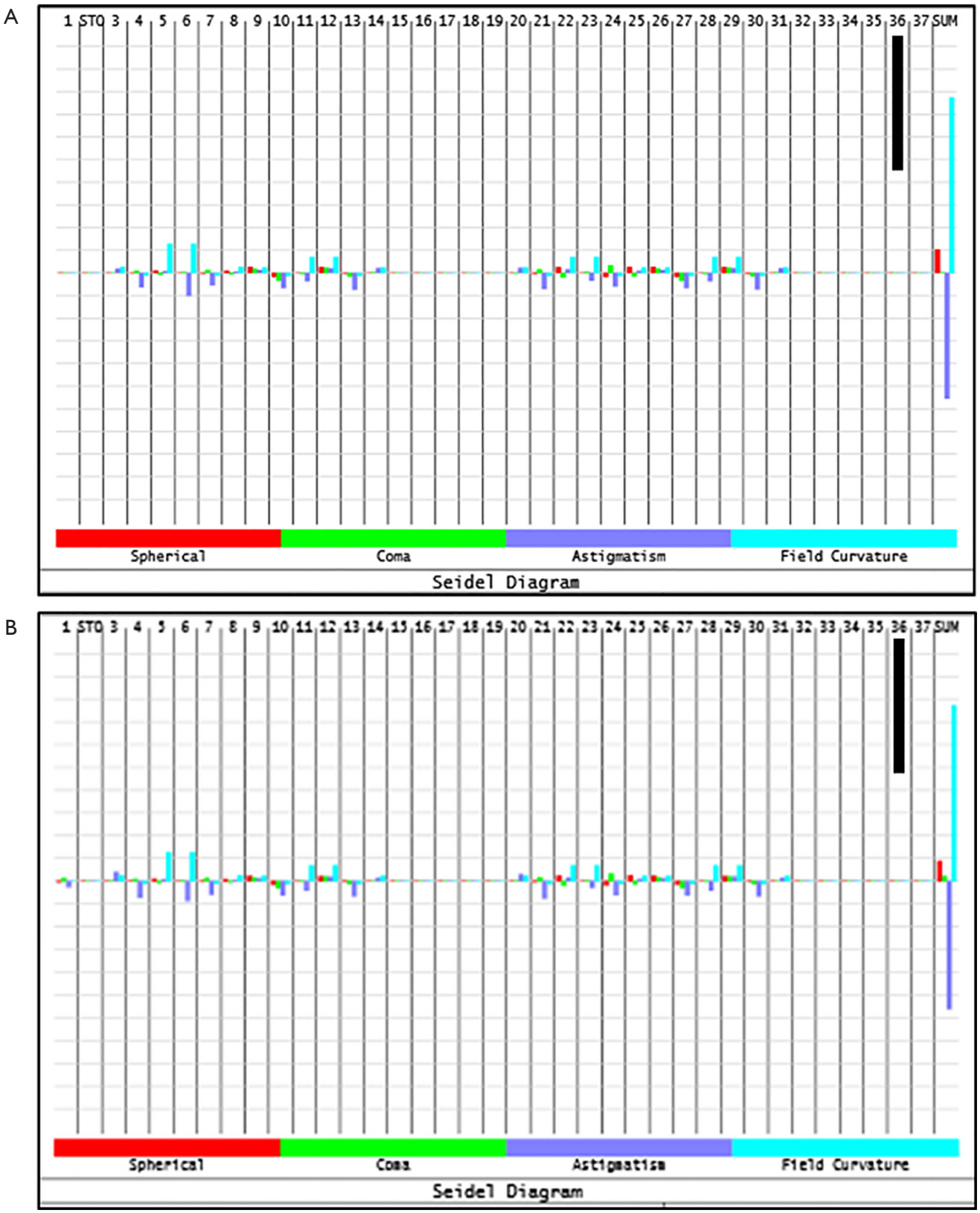

Figure S11 The aberration analysis by Seidel diagram for the layout shown in *Figure S7*. (A) Seidel diagram with mounting medium; (B) Seidel diagram without mounting medium. (Scale bar is 1 μm).

http://dx.doi.org/10.21037/qims-20-806

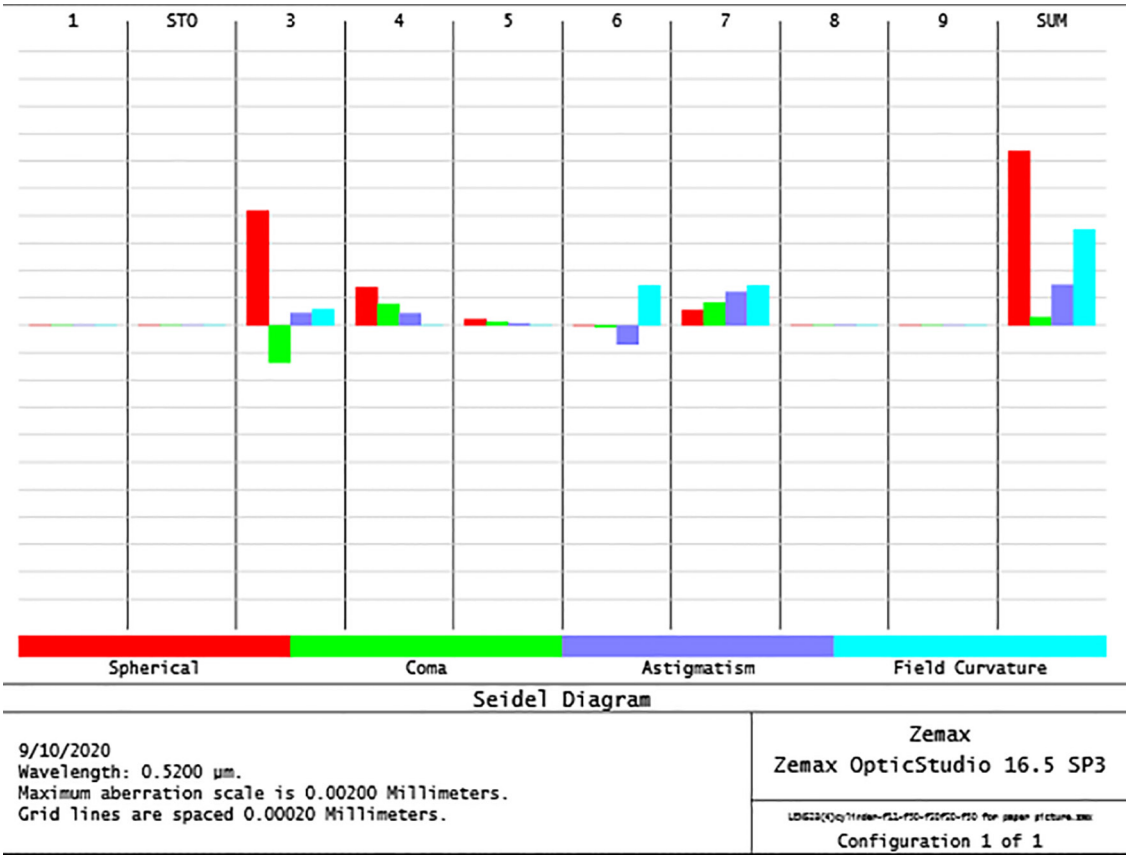

Figure S12 The aberration analysis by Seidel diagram for the layout shown in *Figure S9*.

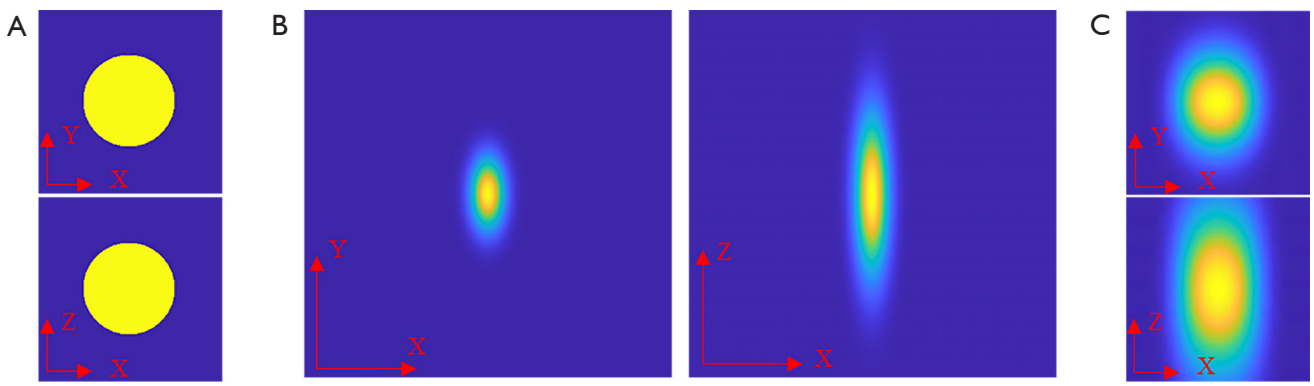

Figure S13 3D convolution of the fluorescent microsphere with system point spread function (PSF). (A) The X-Y and Z-X cross-sections of 3.1 µm fluorescent microsphere; (B) the X-Y and Z-X cross-sections of the theoretical PSF of our system; (C) the maximum intensity projection of the convolution result along the Z and Y direction.

http://dx.doi.org/10.21037/qims-20-806

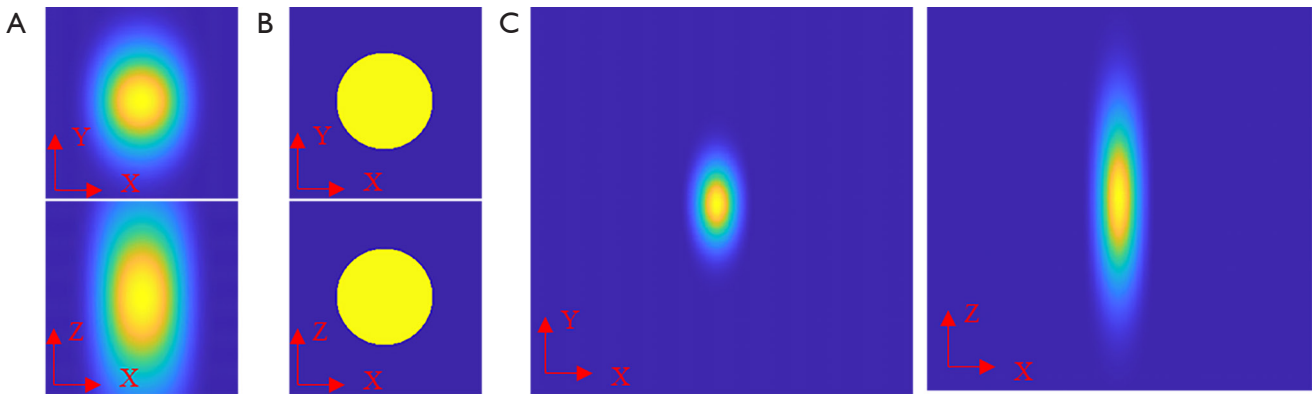

Figure S14 3D deconvolution of the image of the fluorescent microsphere with the fluorescent microsphere itself. (A) The X-Y and Z-X cross-sections of the microsphere image; (B) the X-Y and Z-X cross-sections of 3.1 μm fluorescent microsphere; (C) the maximum intensity projection of the deconvolution result along the Z and Y direction.

Measured resolution	2.5	2.588 5	2.604	2.635	2.666	2.728	2.821	2.852	3.069	3.224
Real resolution	1	1.11	1.162	1.395	1.55	1.64	1.7825	1.86	2.232	2.542
Measured resolution	3.782	4.743	5.58	6.603	7.254	8.215	8.897	9.92	11.16	13.95
Real resolution	3.1	4.34	5.27	6.2	6.975	7.905	8.525	9.765	11.253	13.95

Figure S15 The lookup table of the real and measured resolution along the Z direction.

http://dx.doi.org/10.21037/qims-20-806